2022 International Conference on Unmanned Aircraft Systems (ICUAS)
Dubrovnik, Croatia. June 21-24, 2022

Evenly Weighted Particle Filter for Terrain-referenced Navigation using Gaussian Mixture Proposal Distribution

Junwoo Park and Hyochoong Bang

2022 International Conference on Unmanned Aircraft Systems (ICUAS) | 978-1-6654-0593-5/22/$31.00 ©2022 IEEE | DOI: 10.1109/ICUAS54217.2022.9836197

***Abstract*— The irreversible problematic situation of bootstrap particle filter that it is subject to the weight collapse, is tackled with an evenly weighted setup especially in application to the terrain-referenced navigation problem of unmanned aerial systems. The paper is featured with the Gaussian mixture proposal density taking multimodal noise characteristics of terrain clearance sensor into account. Each particle explores further towards the region of high likelihood in addition to its original motion model, while the amount of transition of the introduced proposal density is calculated from a superposition of a couple of optimal data assimilation methods. Numerical local terrain elevation gradient in conjunction with the parameters that describe the multimodality realize the calculation of transition gain by which the innovation is multiplied. The proposed approach significantly reduces the variance of particle weight and reinforces the diversity of particles by locating them exploiting both the terrain measurement and its noise characteristic.**

I. INTRODUCTION

Terrain-referenced navigation (TRN) is one of the most useful alternative navigation systems to unmanned aerial systems (UAS) [16], the principle of which is to estimate aerial vehicle's position [3] by comparing terrain measurement and digital terrain elevation database (DTED). It becomes especially more valuable when the radio signal of the global navigation satellite system (GNSS) is interfered due to the intended jamming and/or spoofing so that satellite navigation solution is no longer available. TRN problem in general is posed as inferring dynamic states of a vehicle, e.g., position, sequentially from partial information and noisy observations [15] of terrain as depicted in Fig. 1, hence it is mostly associated with the filtering paradigm.

TRN realized by the extended Kalman filter (EKF), however, often fails due to the highly nonlinear and non-Gaussian nature of the problem especially when the locally linearized elevation, thus the slope of the terrain, is not suited for representing the area covered by an error covariance [7] as highlighted in Fig. 1. The main source of the characteristic is the ambiguity [26] of terrain. Therefore, TRN is commonly implemented using nonlinear filters to coop with the nonanalytic terrain elevation. The particle filter (PF) [2] or the point mass filter (PMF) [24] serve fair remedies to the problem with the littlest restrictions by approximating the state space in a numerical fashion.

*This work was not supported by any organization
*Consider for the best student paper award

Junwoo Park and Hyochoong Bang are with the Department of Aerospace Engineering, Korea Advanced Institute of Science and Technology, Daejeon, 34141, Korea {junwoopark, hcbang}@kaist.ac.kr

The PMF, however, whose computation cost increases exponentially, is not extensible to general TRN problems due to the curse of dimensionality, and is only suited for the small models. As a consequence, applications of the standard particle filter (PF) [1], or frequently referred to as a bootstrap PF [2], to the TRN problem is actively investigated [3], [17], [21], [22] owing to its scalability to the multidimensional problems and excellent convergence rate when numerous particles are supported. The idea of using tons of stochastic samples and associated weights to represent probability distribution across the state space has made the PF excel analytic approaches and become universal.

At the same time, however, drawing random and finite samples brings about the defect of the PF as well. When some of the wrong modes are accidentally tracked by particles and high likelihood coincides with the tail of the particle distribution due to the terrain ambiguity, all but a few particles monopolize the weights and the ensemble collapses. This is particularly true when the measurement noise is less variable than the signal noise [15], i.e., peaky likelihood. It becomes more noticeable when the sensors gain more accuracy. Drawing samples from the prior kernel based on the system process model [23], just contributes to the phenomenon since the variance of the weights only increases as shown in [12] with respect to the number of measurement assimilation steps [4]. So-called particle degeneration is easily observed in standard PF. Although the resampling process of sequential importance resampling

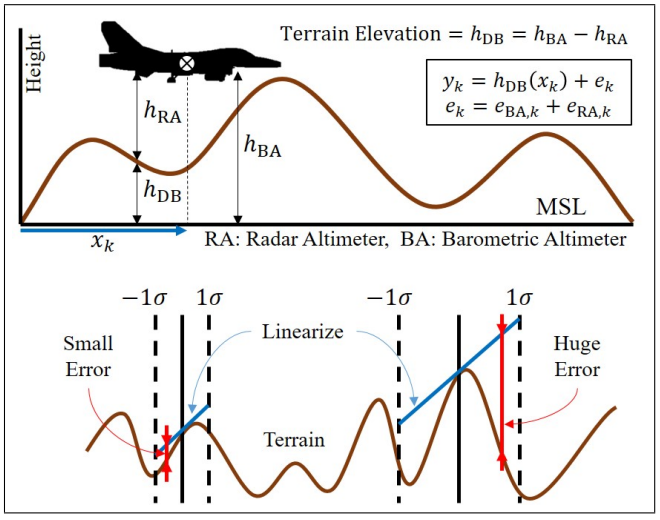

Fig. 1. Principle of the TRN (up), and local terrain linearization error along with error variance (down).

(SIR) setup [25] moderates the problem, resampling from the degenerated particles is nothing but the duplication of the few particles leaving depletion of effective samples, and the filter immediately diverges due to the loss of diversity. Therefore, the ultimate focus should instead be laid on managing evenly weighted particles so that they do not degenerate in the first place, and that they are continuously evenly weighted.

Drawing particles from alternative distributions, i.e., proposal distributions, other than the prior can mitigate the growth of weight variance, since the update of the i^{th} particle's importance weight, w_k^i, is directly influenced by the drawn sample, x_k^i, through the recursion [4],

$$w_k^i \propto w_{k-1}^i \frac{p(y_k|x_k^i)p(x_k^i|x_{k-1}^i)}{q(x_k^i|x_{k-1}^i, y_k)}, \tag{1}$$

where super- and subscripts stand for indices of particle and time respectively, y represents measurement vector, and $q(x_k|x_{k-1}^i, y_k)$ denotes a general form of the proposal distribution with its potential dependency; while the degree of variance reduction (or growth) varies significantly depending upon the choice of q. It is well known that a proposal density which accommodates all the available information up to the time,

$$q(x_k|x_{k-1}^i, y_k) = p(x_k|x_{k-1}^i, y_k) = \frac{p(y_k|x_k)p(x_k|x_{k-1}^i)}{p(y_k|x_{k-1}^i)}, \tag{2}$$

yielding $w_k^i \propto w_{k-1}^i p(y_k|x_{k-1}^i)$, is advocated as the variance of resultant weight is irrelevant to the sampling. It is thus the optimal [1], [5], in terms of maintaining particle diversity and the effective number of samples as large as possible [15]. Despite the theoretical support for the optimal proposal density, however, sampling from it is infeasible in a general sense unless the model is both linear and Gaussian. Moreover, calculation of $p(y_k|x_{k-1}^i)$ involves integration over the entire state space at the k^{th} time step. Hence, numerous studies are devoted to approximating it [6], [13], [14].

Meanwhile, due to the obstacles sticking out of the ground, radio waves of the RA often gets reflected earlier than what's expected. Then an additional mode is introduced in measuring the terrain clearance as highlighted in Fig. 2. Given the fact, the particles of PF-based TRN problem will more likely to degenerate when more precise sensors, such as a laser altimeter [11] whose footprint is narrowed down, or an interferometric radar altimeter [16], [18] that exploits the principle of interferometry, are used; because the concurrence between high-likelihoods and less-weighted regions becomes more probable and less predictable. To avoid the filter divergence in that case, careful management of the particles is again emphasized particularly when sampling those in the prediction step of the PF.

The goal of this study is to demonstrate the effects of Gaussian mixture-based proposal distribution in terms of particle weight variance reduction, especially in application to TRN when the noise of the terrain sensor is multimodal. The distribution is featured with the superposition of a couple of the optimal proposal distributions, which is available only for the linear-Gaussian case, so that more likely samples are drawn taking the terrain measurement as well as its multimodal characteristics into account.

II. Terrain-referenced Navigation using Particle Filter

A. System Model

We consider two-dimensional TRN in this study. With $x = [L, \lambda]^T$ being the state that describes the position of a vehicle, where L and λ denote latitudinal and longitudinal position of a vehicle respectively, state transition function with additive Gaussian noise v_k of known covariance, i.e., $v_k \sim \mathcal{N}(\mathbf{0}, Q_k)$ is given as

$$\begin{aligned} x_k &= f(x_{k-1}) + v_k \\ &= x_{k-1} + \Delta x_k^{\text{INS}} + v_k, \end{aligned} \tag{3}$$

where Δx_k^{INS} denotes position increment acquired by an inertial navigation system (INS) that is modelled as

$$\Delta x_k^{\text{INS}} = x_k^{\text{true}} - x_{k-1}^{\text{true}} + b_k, \tag{4}$$

with b_k being a discrete-time bias added to the true increment. The existence of the bias is not informed to the filter, and only Δx_k^{INS} is exploited as a whole. It is not a sensible model of the INS though, PF uninformed of the bias will linearly diverge without proper correction. The use of such a model implies that the solution scheme detailed in Section IV is scalable to the integrated INS of higher orders that inevitably includes biases.

Denoting the lookup of DTED as h_{DB}, which should be a function of both latitude and longitude, i.e., $h(x) = h_{\text{DB}}(L, \lambda)$, observation model of the problem is given as

$$y_k = h_{\text{DB}}(L_k, \lambda_k) + e_k \tag{5}$$

where e_k is error characteristics of RA, while the most common and naive assumption made on which is that it's Gaussian. The RA measures terrain clearance, while vertical channel of the vehicle is often stabilized with the aid of barometric altimeter (BA) as depicted in Fig. 1. Subtracting clearance from current height does not yield a bias but a small uncertainty. Thus, (5) holds with fair assumption that e_k includes uncertainty of both the RA and the BA, i.e., $\sigma_e = \sqrt{\sigma_{\text{RA}}^2 + \sigma_{\text{BA}}^2}$. Augmenting σ_e with DTED noise, σ_{DB}, is also favored.

B. Multimodality of the Radar Altimeter

However, the zero-mean Gaussian assumption of e_k only holds for the ideal case. RA typically measures any echo from the ground reflection whose sources are often indistinguishable, thus it is subject to anomalies. Especially when the vehicle is flying over unregistered natural objects such as treetops, vegetated areas; or artifacts such as newly-built landmarks, radar beams get scattered off the canopy of the obstacles [9] instead of being reflected from the true elevation. In that case, terrain measurement and elevation stored in DTED do not coincide, and additional mode centered at the

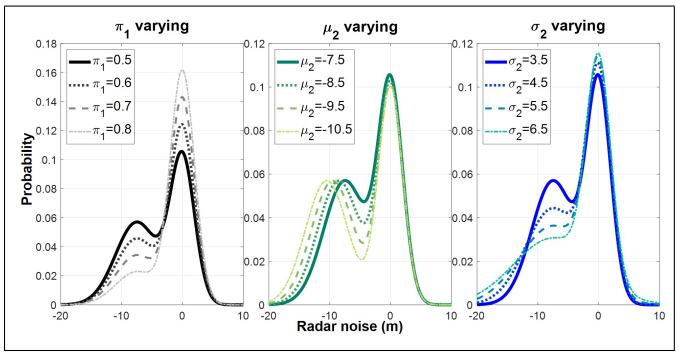

Fig. 2. Typical error characteristics of RA. Three solid lines are identical with $\pi_1 = 0.5, \mu_2 = -7.5, \sigma_1 = 2, \sigma_2 = 3.5$; see (6)

negative value[1] is developed in RA. One study [10] suggests a simple, but effective solution to the problem by modelling the measurement noise as a sum of multiple Gaussian modes as

$$p_e(\cdot) \sim \sum_{j=1}^{N_m} \pi_j \mathcal{N}\left(\mu_j, \sigma_j^2\right), \tag{6}$$

and experimentally shows that the model is realistic. Here, N_m denotes the number of modes which is 2 in this study, π_1 is the ratio of the unscattered signal, i.e., reflected from the actual elevation, yielding $\pi_2 = 1 - \pi_1$. μ_j and σ_j are the mean and the standard deviation of j^{th} mode, while obviously $\mu_1 = 0$. Typical error characteristics of RA is sketched in Fig. 2, using various sets of parameters.

The magnitude of μ_2 is roughly equal to the average tree height within the region of interest [9]. Although all the parameters in (6) may vary upon several conditions, such as radar cross-section (RCS) of canopies, leaf-area index (LAI) [19] of the footprint, and/or air humidity [20], it is assumed that they are fixed and known in advance based primarily on the LAI. Commonly used C-banded RA, whose wavelength is not short enough to penetrate leaves, supports the idea.

C. Principle of the Particle Filter

The PF, which is a Monte Carlo approach of performing Bayesian estimation, approximates the state distribution at k^{th} time step, e.g., a posterior, using N random samples and their corresponding scalar weights, $\{x_k^i, w_k^i\}_{i=1}^N$, as

$$p(x_k|y_{1:k}) \approx \sum_{i=1}^{N} w_k^i \delta(x_k - x_k^i) \tag{7}$$

where $\delta(\cdot)$ is the Dirac delta function and $s_{1:k}$ denotes the sequence of signals $s_1, s_2, \cdots, s_k$, so that the integration of a function of interest, g, over the state space $\mathcal{X}_k$ is approximated as

$$\int_{\mathcal{X}_k} g(x_k) p(x_k|y_{1:k}) dx_k \approx \sum_{i=1}^{N} w_k^i g(x_k^i), \tag{8}$$

[1]becomes positive when subtracted from BA

particular example of which is the minimum mean square error (MMSE) estimate, i.e., expectation, that is

$$x_k^{\text{MMSE}} = \int_{\mathcal{X}_k} x_k p(x_k|y_{1:k}) dx_k \approx \sum_{i=1}^{N} w_k^i x_k^i. \tag{9}$$

Based on the general Bayesian update recursion:

$$\begin{aligned} p(x_k|y_{1:k-1}) &= \int_{\mathcal{X}_{k-1}} p(x_k|x_{k-1}) p(x_{k-1}|y_{1:k-1}) dx_{k-1} \\ p(x_k|y_{1:k}) &= \frac{p(y_k|x_k) p(x_k|y_{1:k-1})}{\int_{\mathcal{X}_k} p(y_k|x_k) p(x_k|y_{1:k-1}) dx_k}, \end{aligned} \tag{10}$$

prediction step of the PF is to occupy the state space by drawing samples $\{x_k^i\}_{i=1}^N$ from the proposal distribution of our choosing, $q(x_k|x_{k-1}^i, y_k)$, and compensate for the mismatch using importance weight as

$$w_{k|k-1}^i \propto w_{k-1}^i \frac{p(x_k^i|x_{k-1}^i)}{q(x_k^i|x_{k-1}^i, y_k)}, \tag{11}$$

where the conventional notation is used in representing temporal dependency as a subscript. It is followed by the measurement update step based on the Bayes rule as

$$w_k^i = \frac{w_{k|k-1}^i p(y_k|x_k^i)}{\sum_{j=1}^N w_{k|k-1}^j p(y_k|x_k^j)}, \tag{12}$$

combination of which with (11) completes (1). The most obvious and practical choice of q is the prior, $p(x_k|x_{k-1}^i) = \mathcal{N}\left(x_k - f(x_{k-1}^i), Q_k\right)$ that nullifies (11).

Meanwhile, particles are optionally resampled based on the degree of depletion, which is also known as the effective number of samples, when the following condition holds for the approximated value of the indicator:

$$\hat{N}_{\text{eff}} = \frac{1}{\sum_{i=1}^N (w_k^i)^2} < \eta N, \tag{13}$$

where $\eta \in (0, 1]$ is a predetermined variable denoting the ratio for the threshold. After resampling, all the particles are equally weighted. Readers are referred to [8] for instance, for common resampling algorithm and further details of the PF other than recalled herein.

III. Optimal Proposal Density using Local Linearization

One has absolute freedom in selecting distributions from which to draw particles other than the process model (3). A model [4] of the form:

$$x_k = f(x_{k-1}) + K_k \{y_k - h(f(x_{k-1}))\} + \hat{v}_k, \tag{14}$$

for instance, pushes the particle toward the given measurement as much as the innovation multiplied by some gain K_k. Note that the stochastic part, $\hat{v}_k$, differs from v_k. This kind of forcing will bring higher likelihoods taking the measurement into account, while proposal weight in (11) should be traded off as the particles have drifted away from the original model equation (3). The existence of the proposal distribution that balances the both by tuning the gain is

easily anticipated. If we further assume that $e_k \sim \mathcal{N}(\mathbf{0}, R_k)$, utilization of another optimal data assimilation method, i.e., the EKF, provides rational approximation [12], [13], [15] to the optimal proposal distribution (2) as

$$q(x_k|x_{k-1}^i, y_k) = \mathcal{N}\left(f(x_{k-1}^i) + K_k^i(y_k - \hat{y}_k^i), \left(I - K_k^i H_k^i\right) Q_{k-1}\right), \tag{15}$$

given that $\hat{y}_k^i = h(f(x_{k-1}^i))$. Here, H_k^i is a locally linearized measurement model,

$$H_k^i = \left.\frac{\partial h(x_k))}{\partial x_k}\right|_{x_k = f(x_{k-1}^i)}, \tag{16}$$

while the rationale behind (15) is the usual EKF equations:

$$\begin{aligned} \hat{x}_{k-1|k-1} &\sim \mathcal{N}(x_{k-1}^i, \mathbf{0}) \\ \hat{x}_{k|k-1} &= f(x_{k-1}^i) \\ P_{k|k-1} &= Q_{k-1} \\ K_k^i &= Q_{k-1} H_k^{i,T} \left(H_k^i Q_{k-1} H_k^{i,T} + R_k\right)^{-1} \\ \hat{x}_{k|k} &= \hat{x}_{k|k-1} + K_k^i(y_k - h(\hat{x}_{k|k-1})) \\ P_{k|k} &= \left(I - K_k^i H_k^i\right) Q_{k-1}, \end{aligned} \tag{17}$$

considering each particle at the prior distribution as a non-covariant deterministic estimate. As a consequence, weight update (1) is substituted with

$$w_k^i \propto w_{k-1}^i \mathcal{N}(y_k - h(f(x_{k-1}^i)), H_k^i Q_{k-1} H_k^{i,T} + R_k), \tag{18}$$

using innovation covariance matrix.

Note that (15) becomes indeed the optimal proposal distribution when the problem is linear and Gaussian [4], [13], and $\hat{v}_k$ of (14) is then from $\mathcal{N}(\mathbf{0}, Q_{k-1} - K_k^i H_k^i Q_{k-1})$ for each particle. However, e_k of this study is not unimodal as described in Section II-B. Then, there is a fair chance that the weights of particles vary much when they were sampled from (15) by approximating (6) as a single Gaussian of huge variance. The strategy in this study is to superpose a couple of (15) by fully exploiting (6). Following section details the proposed method and presents numerical analyses.

IV. Evenly Weighted Particle Filter for Terrain-referenced Navigation

A. Gaussian Mixture-based Proposal Distribution

Given the error characteristics of RA as in (6), we consider sampling a particle from the Gaussian mixture proposal distribution of the form:

$$q(x_k|x_{k-1}^i, y_k) = \sum_{j=1}^{N_m} \pi_j \mathcal{N}\left(f(x_{k-1}^i) + K_k^{i,(j)} \tilde{y}_k^{i,(j)}, P_{k|k}^{(j)}\right), \tag{19}$$

where for $j \in \{1, 2\}$,

$$\begin{aligned} K_k^{i,(j)} &= Q_{k-1} H_k^{i,T} \left(H_k^i Q_{k-1} H_k^{i,T} + \sigma_j^2\right)^{-1} \\ P_{k|k}^{(j)} &= \left(I - K_k^{i,(j)} H_k^i\right) Q_{k-1} \\ \tilde{y}_k^{i,(j)} &= y_k - \hat{y}_k^i + \mu_j, \end{aligned} \tag{20}$$

according to (17). Here, the i^{th} particle is nudged towards the given measurement considering the j^{th} mode of e by the amount of $K_k^{i,(j)}$ multiplied by the innovation $\tilde{y}_k^{i,(j)}$. The addition of μ_j, not subtraction, is due to the relationship between (5) and RA measurement. Each cluster of the Gaussian mixture-based proposal distribution associates with each mode of (6). Based on the rationale introduced in Section III, each particle is stochastically pushed towards a more probable region depending on the result of a Bernoulli trial where the probability for one of the binary outcomes is the same as the chance of RA measuring signals from the actual terrain.

After a x_k^i is sampled from (19), (1) is exploited as a whole for the weight update as

$$w_k^i \propto w_{k-1}^i \times \frac{p_e\left(y_k - h(x_k^i)\right) p_v\left(x_k^i - f(x_{k-1}^i)\right)}{\sum_j \pi_j \mathcal{N}\left(x_k^i; f(x_{k-1}^i) + K_k^{i,(j)} \tilde{y}_k^{i,(j)}, P_{k|k}^{(j)}\right)} \tag{21}$$

where $p_e(\cdot)$ is from (6) and $p_v(\cdot) \sim \mathcal{N}(\mathbf{0}, Q_k)$.

Meanwhile, the calculation of (20) necessitates that of (16). It is numerically calculated in this study using DTED as

$$H = \begin{bmatrix} \frac{\partial h}{\partial L} \\ \frac{\partial h}{\partial \lambda} \end{bmatrix} = \begin{bmatrix} \frac{h_{\text{DB}}(L + \Delta L, \lambda) - h_{\text{DB}}(L, \lambda)}{\Delta L} \\ \frac{h_{\text{DB}}(L, \lambda + \Delta\lambda) - h_{\text{DB}}(L, \lambda)}{\Delta\lambda} \end{bmatrix}, \tag{22}$$

where ΔL and Δl denote small deviation of latitude, and longitude respectively. The worldwide DTED available from shuttle radar topology mission (SRTM) [27] whose resolution is around 1arcsec, i.e., 30m, is utilized and bilinear interpolation method is applied when terrain elevation at a subgrid position is queried. Authors also found that following variant of (22)

$$\begin{aligned} \frac{\partial h}{\partial L} &= \frac{h_{\text{DB}}(L + \Delta L, \lambda) - h_{\text{DB}}(L - \Delta L, \lambda)}{2\Delta L} \\ \frac{\partial h}{\partial \lambda} &= \frac{h_{\text{DB}}(L, \lambda + \Delta\lambda) - h_{\text{DB}}(L, \lambda - \Delta\lambda)}{2\Delta\lambda}, \end{aligned} \tag{23}$$

is also valid in calculating (16), and often provides better numerical stability. For further details of terrain slope estimation, such as a stochastic linearization, readers are referred to [7].

B. Numerical Simulation

To demonstrate the effect of the proposed method in regulating the growth of particle weight variance compared to the standard setting, it is tested on two trajectories. The terrain elevation varies significantly along the first trajectory, hence named a rough trajectory, while the second trajectory has less changing terrain and we call it a smooth trajectory. Both trajectories along with the terrain distribution are illustrated in Fig. 3.

At the initial step, particles get scattered based on a broad distribution that is centered at somewhere else than the true initial position, i.e., $x_0 \sim \mathcal{N}(x_0^{\text{true}} + e_0, P_0)$, while P_0 is large enough so that x_0^{true} is within the coverage of the particles.

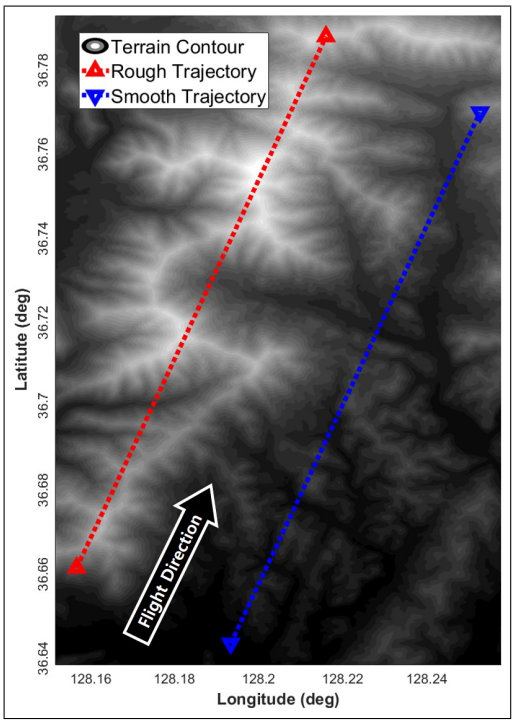

Fig. 3. Terrain contour plot and simulation trajectories

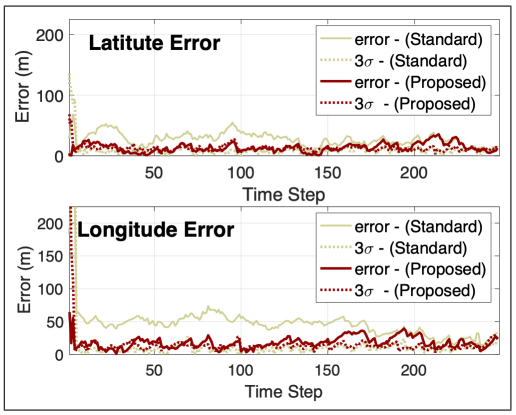

Fig. 4. Time history of the estimation errors for the rough trajectory

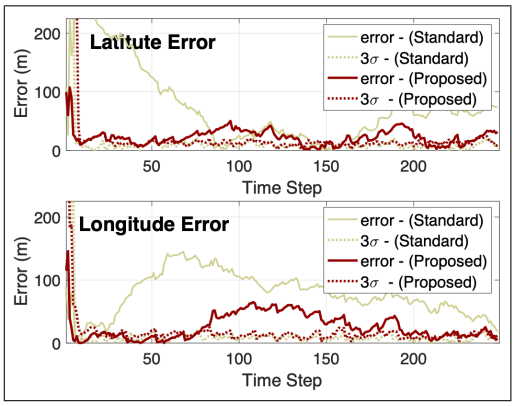

Fig. 5. Time history of the estimation errors for the smooth trajectory

A complete list of the parameters used in the simulation is given in Table I.

Fig. 4 shows a time history of the position estimation errors when the standard setting and the proposed method is used for the rough trajectory, while Fig. 5 is the same for the smooth trajectory. These errors along with their covariance primarily present the convergence of the filter. As the smooth, i.e., less varying, terrain is less distinguishable from the surroundings, it becomes less observable as shown in Fig. 5 compared to Fig. 4.

Fig. 6 shows a time history of the variance of particle weights when the rough trajectory is exploited, while Fig. 7 is the same for the smooth trajectory. In both the graphs, circles are marked when the resampling is triggered under the condition of $\eta = 0.8$. Note that they mostly correspond to the peaks of weight variance. From both the trajectories, the resampling function is called less frequently in the proposed method. The weight variance of the proposed method is maintained low across the simulation, which is even three to four times smaller than the standard setting in terms of the average value.

To exaggerate the effect, η is then set low to 0.2 so that the resampling is less triggered, and the result is shown in Fig. 8. By doing so healthiness of the particles, that is the littleness of the variance of particle weights, rely more on the proposal distribution. Since the particles get resampled fewer times, weight variance tends to increase in both the trajectories compared to the cases when $\eta = 0.8$. Nevertheless, the proposed method effectively suppresses the growth of the variance particle weights even with the little aid of the resampling process, whereas in standard setting it continuously rises especially in the early stage of the filter where it is prone to diverge.

Peaks of Fig. 6∼8 is due to the linearization mismatch, just as delineated in Fig. 1, in the vicinity of terrain bumps. It happens when the steep terrain change is anticipated in (22) where in fact it is not, or vice versa. Then, each particle is pushed further than, or not as far as, it should be. In order to fully suppress the growth of weight variance in that cases, careful terrain slope estimation should be supported.

TABLE I
SIMULATION PARAMETERS

Parameter	Value	Remark
μ_1, μ_2	0m, -7.5m	(6)
σ_1, σ_2	2m, 3.5m	(6)
π_1, π_2	0.5, 0.5	(6)
b_k	$\begin{bmatrix} 2m \\ 2m \end{bmatrix}$	(4)
Q	$\begin{bmatrix} 2.5m & 0 \\ 0 & 2.5m \end{bmatrix}^2$	(3)
$\|e_0\|, P_0$	150m, $\begin{bmatrix} 150m & 0 \\ 0 & 150m \end{bmatrix}^2$	x_0
N	50	(7)
η	0.8, 0.2	(13)
$\Delta L, \Delta\lambda$	5m	(16)

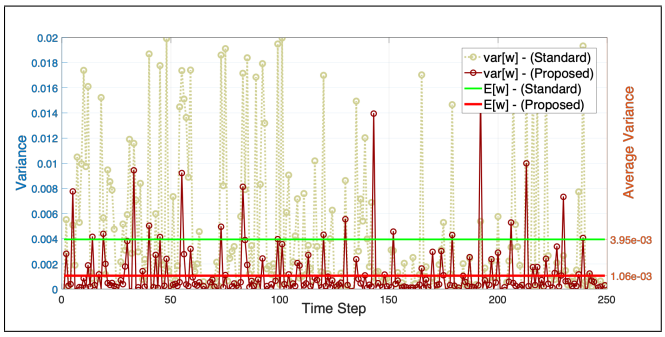

Fig. 6. Time history of the weight variance for the rough trajectory

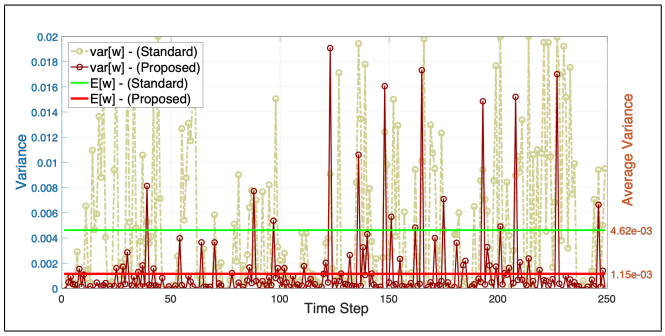

Fig. 7. Time history of the weight variance for the smooth trajectory

V. Conclusion

The proposal distribution based on the Gaussian mixture is considered in this study where each mode of the distribution takes each peak of RA's measurement likelihood into account. As it appears in Fig. 4, the proposed method does no harm to the filter convergence or even increases the performance by maintaining effective particles. What's more important is that the internal statistic gets improved. The smoother variance growth is observed on both rough and smooth terrains compared to the standard setting. The primary conclusion derived from the observation is that it can keep healthy and meaningful particles longer even under the defensive use of resampling.

In application to the UAS, if the regions of flight are determined before the departure, it is possible to plan in advance for the particle sampling strategy based on the LAI index of the regions and thus the multimodal characteristics of RA. One of our next moves is to demonstrate the effect of the proposed idea expanded to higher-order navigation problems where PF, especially in its standard setup, has difficulties in converging.

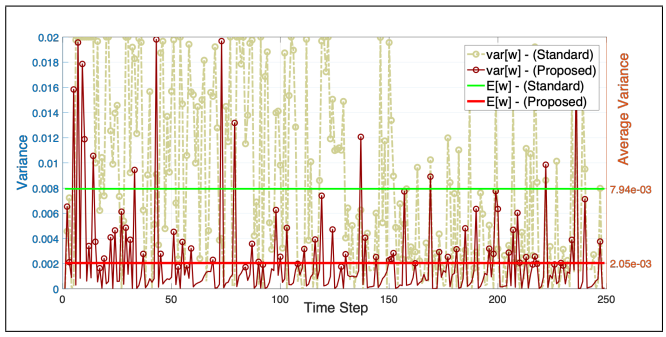

Fig. 8. Time history of the weight variance for the rough trajectory when $\eta = 0.2$

References

[1] Doucet, A., De Freitas, N., Gordon, N. & Others Sequential Monte Carlo methods in practice. (Springer,2001)

[2] Gordon, N., Salmond, D. & Smith, A. Novel approach to nonlinear/non-Gaussian Bayesian state estimation. *IEE Proceedings F-radar And Signal Processing*. **140**, 107-113 (1993)

[3] Nordlund, P. & Gustafsson, F. Marginalized particle filter for accurate and reliable terrain-aided navigation. *IEEE Transactions On Aerospace And Electronic Systems*. **45**, 1385-1399 (2009)

[4] Van Leeuwen, P., Künsch, H., Nerger, L., Potthast, R. & Reich, S. Particle filters for high-dimensional geoscience applications: A review. *Quarterly Journal Of The Royal Meteorological Society*. **145**, 2335-2365 (2019)

[5] Snyder, C., Bengtsson, T. & Morzfeld, M. Performance bounds for particle filters using the optimal proposal. *Monthly Weather Review*. **143**, 4750-4761 (2015)

[6] Pitt, M. & Shephard, N. Filtering via simulation: Auxiliary particle filters. *Journal Of The American Statistical Association*. **94**, 590-599 (1999)

[7] Mok, S., Choi, M. & Bang, H. Performance comparison of nonlinear estimation techniques in terrain referenced navigation. *2011 11th International Conference On Control, Automation And Systems*. pp. 1244-1249 (2011)

[8] Arulampalam, M., Maskell, S., Gordon, N. & Clapp, T. A tutorial on particle filters for online nonlinear/non-Gaussian Bayesian tracking. *IEEE Transactions On Signal Processing*. **50**, 174-188 (2002)

[9] Park, J., Park, Y. & Park, C. Parameter estimation of radar noise model for terrain referenced navigation using a new EM initialization method. *IEEE Transactions On Aerospace And Electronic Systems*. **56**, 107-112 (2019)

[10] Schon, T., Gustafsson, F. & Nordlund, P. Marginalized particle filters for mixed linear/nonlinear state-space models. *IEEE Transactions On Signal Processing*. **53**, 2279-2289 (2005)

[11] Han, K., Sung, C., Yu, M. & Park, C. Performance improvement of laser TRN using particle filter incorporating gaussian mixture noise model and novel fault detection algorithm. *Proceedings Of The 31st International Technical Meeting Of The Satellite Division Of The Institute Of Navigation (ION GNSS+ 2018)*. pp. 3317-3326 (2018)

[12] Doucet, A. On sequential simulation-based methods for Bayesian filtering. (Citeseer,1998)

[13] Doucet, A., Godsill, S. & Andrieu, C. On sequential Monte Carlo sampling methods for Bayesian filtering. *Statistics And Computing*. **10**, 197-208 (2000)

[14] Van Der Merwe, R., Doucet, A., De Freitas, N. & Wan, E. The unscented particle filter. *Advances In Neural Information Processing Systems*. **13** (2000)

[15] Gustafsson, F. Particle filter theory and practice with positioning applications. *IEEE Aerospace And Electronic Systems Magazine*. **25**, 53-82 (2010)

[16] Park, J., Kim, Y. & Bang, H. A new measurement model of interferometric radar altimeter for terrain referenced navigation using particle filter. *2017 European Navigation Conference (ENC)*. pp. 57-64 (2017)

[17] Merlinge, N., Dahia, K. & Piet-Lahanier, H. A box regularized particle filter for terrain navigation with highly non-linear measurements. *IFAC-PapersOnLine*. **49**, 361-366 (2016)

[18] Kim, Y., Park, J. & Bang, H. Terrain-referenced navigation using an interferometric radar altimeter. *NAVIGATION, Journal Of The Institute Of Navigation*. **65**, 157-167 (2018)

[19] Rosen, P., Hensley, S., Zebker, H., Webb, F. & Fielding, E. Surface deformation and coherence measurements of Kilauea Volcano, Hawaii, from SIR-C radar interferometry. *Journal Of Geophysical Research: Planets*. **101**, 23109-23125 (1996)

[20] Prevot, L., Champion, I. & Guyot, G. Estimating surface soil moisture and leaf area index of a wheat canopy using a dual-frequency (C and

X bands) scatterometer. *Remote Sensing Of Environment*. **46**, 331-339 (1993)
[21] Murangira, A., Musso, C. & Dahia, K. A mixture regularized rao-blackwellized particle filter for terrain positioning. *IEEE Transactions On Aerospace And Electronic Systems*. **52**, 1967-1985 (2016)
[22] Teixeira, F., Quintas, J., Maurya, P. & Pascoal, A. Robust particle filter formulations with application to terrain-aided navigation. *International Journal Of Adaptive Control And Signal Processing*. **31**, 608-651 (2017)
[23] Teixeira, F., Pascoal, A. & Maurya, P. A novel particle filter formulation with application to terrain-aided navigation. *IFAC Proceedings Volumes*. **45**, 132-139 (2012)
[24] Alspach, D. & Sorenson, H. Nonlinear Bayesian estimation using Gaussian sum approximations. *IEEE Transactions On Automatic Control*. **17**, 439-448 (1972)
[25] Rubin, D. Using the SIR algorithm to simulate posterior distributions. *Bayesian Statistics*. **3** pp. 395-402 (1988)
[26] Kim, Y., Hong, K. & Bang, H. Utilizing out-of-sequence measurement for ambiguous update in particle filtering. *IEEE Transactions On Aerospace And Electronic Systems*. **54**, 493-501 (2017)
[27] Farr, T. & Kobrick, M. Shuttle Radar Topography Mission produces a wealth of data. *Eos, Transactions American Geophysical Union*. **81**, 583-585 (2000)